

## THE ABUNDANCE OF $^{14}\text{N}$ AT THE COSMIC-RAY SOURCE: A STUDY USING NEW FRAGMENTATION CROSS SECTIONS

M. GUPTA AND W. R. WEBBER

Space Science Center, University of New Hampshire  
 Received 1987 December 11; accepted 1988 October 25

### ABSTRACT

The long-standing nitrogen puzzle in Galactic cosmic rays is reexamined. New cross sections measured by the New Hampshire group at the BEVALAC are used along with a new cross section program to estimate unmeasured cross sections. These cross sections are then incorporated into a Galactic propagation program to calculate the interstellar production of boron and nitrogen. The leaky box approximation is used to describe this propagation, and the solar modulation factor, source abundance, and escape path length are varied. It is found that, using the new cross-sections, the escape path length needs to be increased by about 18% over previous values to  $\lambda_e = 23.8 \beta R^{-0.60}$  for a rigidity  $R > 4.5$  GV and  $\lambda_e = 9.7 \beta \text{ g cm}^{-2}$  for  $R < 4.5$  GV. A low-energy  $\beta$ -dependence is required to fit both the B/C and N/O ratios. With the new path length the predicted B/C and N/O elemental ratios closely fit the observations at all energies, but only in conjunction with a  $^{14}\text{N}/\text{O}$  source ratio equal to  $3.8\% \pm 1\%$ . This is corroborated by the  $^{14}\text{N}/\text{O}$  isotopic ratio predictions, which now reasonably well fit the observations at all energies. The fit for the  $^{15}\text{N}/\text{O}$  isotopic ratio is also improved and is consistent with a source  $^{15}\text{N}/\text{O}$  ratio  $\gtrsim 1\%$  although some systematic uncertainties still exist. An examination of the abundance excess of the neutron-rich isotopes  $^{22}\text{Ne}$ ,  $^{25}\text{Mg}$ , and  $^{26}\text{Mg}$  in cosmic rays shows that they are almost exactly balanced by the depletion of  $^{14}\text{N}$  relative to the solar coronal abundances, suggesting that these abundance differences may be related.

*Subject headings:* cosmic rays: abundances

### I. INTRODUCTION

The importance of nitrogen in nucleosynthetic and other astrophysical phenomena has long been recognized. Accurate determinations of the source abundance of  $^{14}\text{N}$  in cosmic rays have been difficult for various reasons, so that the source abundance of  $^{14}\text{N}$  has remained largely a controversial issue. Since interstellar fragmentation alone creates over 80% of all cosmic-ray N observed at Earth, uncertainties in cross-sectional data have been primarily responsible for the uncertainties in estimating this source abundance. Two problems have arisen when comparing predictions with experiment that we seek to resolve in this paper: First, using previous cross sections, the predicted  $^{15}\text{N}/\text{O}$  ratio is considerably less than that observed at low energies, for an interstellar path length adjusted to yield a good fit to the B/C ratio (e.g., Webber 1983; Meyer 1985*a, b*; Gupta 1987). The assumption here is that both the  $^{15}\text{N}/\text{O}$  and the B/C ratios should be fit simultaneously, since both  $^{15}\text{N}$  and B are purely secondaries. Second, the source abundance for  $^{14}\text{N}$  derived from both the high- and low-energy measurements of the isotopic  $^{14}\text{N}/\text{O}$  ratio must be the same as that determined from the elemental N/O ratio. The elemental N/O ratio has been accurately determined over a wide range of energies and yields a source abundance  $\sim 6\%$  at both high and low energies (Meyer 1985*a, b*). Direct isotopic  $^{14}\text{N}/\text{O}$  ratio measurements yield a source abundance for  $^{14}\text{N}/\text{O} = 2\%–3\%$  at low energies and  $^{14}\text{N}/\text{O} = 5\%–7\%$  at high energies using previous cross sections (Webber 1983; Meyer 1985*a, b*). The low-energy isotopic measurements are therefore inconsistent with results obtained from the elemental N/O data.

In this paper we reexamine these problems using a new, improved set of spallation cross sections.

### II. THE LEAKY BOX MODEL AND THE PROPAGATION PROGRAM USED

A version of the propagation program created by Comstock (1969) is used throughout. The “leaky box” model incorporating a purely exponential distribution of path lengths is used. The results of this study are not dependent on the exact shape of the path length distribution. The form of the transport equation, following Gloeckler and Jokipii (1969), in terms of kinetic energy per nucleon,  $T$ , is

$$\frac{\partial}{\partial T} \left[ \left( \frac{\partial T}{\partial x} \right)_i J_i(T) \right] + \left( \frac{1}{\lambda_e} + \frac{\sigma_i}{M_p} \right) J_i(T) = q_i(T) + \sum_{\substack{k \neq i \\ k > i}} \frac{1}{M_p} \int_0^\infty J_k(T') \sigma_{ki}(T, T') dT' F(T, T'), \quad (1)$$

where  $x$  is the amount of matter traversed in  $\text{g cm}^{-2}$ ,  $\sigma_i$  is the nuclear destruction cross section of the nucleus  $i$ ,  $\sigma_{ki}$  is the cross section for forming the nucleus  $i$  at energy  $T$  from the parent  $k$  ( $k > i$ ), with energy  $T'$  in an ISM of pure hydrogen, with density  $n_H$ ,  $\lambda_e = c\beta M_p n_H \tau_e$ ,  $\tau_e$  is the leakage lifetime,  $q_i$  is the source function, and  $M_p$  is the hydrogen mass in grams.

In terms of the differential intensity  $J_i(T)$ , we have for a solution

$$J_i(T) = \int_0^\infty P(x) j_i(x, T) dx, \quad (2)$$

where  $j_i(x, T)$  is the propagation function defined in Gupta (1987) along with a detailed derivation.  $P(x)$  is the path length distribution which for a uniform source distribution is an exponential  $P(x) = (c_0/x_0) \exp(-x/x_0)$ .

This treatment is analogous to an unbounded uniform source distribution (Fichtel and Reames 1968; Comstock 1969). In calculations done by the program, the kinematical distribution function  $F(T, T')$  in equation (1) is replaced by  $\delta(T - T')$ , a good approximation in high-energy spallation reactions of heavy nuclei on hydrogen in which the velocity of the fragments is close to that of the parent.

In the above framework, the general method of calculation is as follows: Individual species are propagated in pure H, and secondary abundances are determined for specific propagation parameters and cross sections read in from a separate input file. The parameters to be varied in an attempt to fit measured data are as follows:

- The rigidity-dependent escape path length (henceforth  $\lambda_e$  for convenience).
- The solar modulation factor ( $\phi$ ) determined in the "force-field" approximation of Gleeson and Axford (1968).
- The source abundances.

The source function input spectra for all species are assumed to be power laws in rigidity, the value adopted here being  $\gamma = -2.2$ , consistent with that adopted by Engelmann *et al.* (1983, 1985).

### III. THE CROSS SECTIONS

Table 1 shows the Saclay, Tsao and Silberberg (1979, hereafter TS) partial fragmentation cross sections into B and N, modified by the introduction of the key cross sections by the University of New Hampshire (UNH) group available in 1982 and used in earlier calculations by Koch-Miramond *et al.* (1983). These are the decayed cross sections. The unmeasured semiempirical cross sections from the TS formula that are used in this calculation are stated to have rms errors of  $\sim 35\%$ , primarily due to the limited cross-section data available. Accurate cross sections for many of these reactions have now been measured over the last few years at the BEVALAC by the UNH group (e.g., Webber 1984; Webber and Kish 1985; Webber, Kish, and Schrier 1987; Webber 1987a) in H targets. These measurements, performed with 12 different source nuclei ranging from  $^{12}\text{C}$  to  $^{58}\text{Ni}$ , cover over 90% of all cosmic-ray nuclei initially at the source or  $\sim 70\%$  of all cosmic-ray nuclei arriving at Earth. This includes the latest, not yet published, cross-section measurements using  $^{14}\text{N}$ ,  $^{23}\text{Na}$ ,  $^{26}\text{Mg}$ , and  $^{27}\text{Al}$  beams. A total of over 300 individual isotope cross sections have been measured at 600 MeV nucleus $^{-1}$  for secondary fragments with  $Z_f > 0.6$  times the beam charge,  $Z_i$ . The measurements of elemental cross sections have been made over a large range of energies from 300 MeV nucleus $^{-1}$  up to 1600 MeV nucleus $^{-1}$ . Also, a new, much improved, semiempirical cross-section program has been developed (Webber 1987b) for all elements with  $A = 7-60$ , including neutron-rich parents, which predicts the cross sections in H. The rms accuracy of this formula is 10% or better for cross sections where measurements are available (including the new neutron-rich parents) for energies greater than 150 MeV nucleus $^{-1}$  and is a factor of greater than 3 improvement over the TS formula mentioned above (Webber 1988). Both the directly measured and predicted UNH cross sections are shown at an energy of 600 MeV nucleus $^{-1}$  in Table 1. It is seen that the new UNH values for the production of  $^{15}\text{N}$  are systematically greater than the corresponding TS values. The UNH cross sections into B on the other hand tend to be systematically smaller for all charges greater than oxygen. Similar differences apply at other energies.

TABLE 1  
DECAYED PARTIAL CROSS SECTIONS AT 600 MeV NUCLEUS $^{-1}$  <sup>a</sup>

	BORON				NITROGEN			
	$^{10}\text{B}$		$^{11}\text{B}$		$^{14}\text{N}$		$^{15}\text{N}$	
	S	UNH <sup>b</sup>	S	UNH <sup>b</sup>	S	UNH <sup>b</sup>	S	UNH <sup>b</sup>
$^{11}\text{B}$ .....	28.6	28.6	...	...	...	...	...	...
$^{12}\text{C}$ .....	19.0 <sup>c</sup>	19.0 <sup>d</sup>	56.0 <sup>c</sup>	56.0 <sup>d</sup>	...	...	...	...
$^{13}\text{C}$ .....	13.4	6.0-	62.2	37.9-	...	...	...	...
$^{14}\text{N}$ .....	22.5	15.1-	31.4	31.4	...	...	...	...
$^{15}\text{N}$ .....	10.8	3.8-	50.0	25.0-	68.3	64.1	...	...
$^{16}\text{O}$ .....	10.7 <sup>c</sup>	10.7 <sup>d</sup>	27.0 <sup>c</sup>	M27.0 <sup>d</sup>	42.0 <sup>c</sup>	42.0 <sup>d</sup>	63.0 <sup>c</sup>	63.0 <sup>d</sup>
$^{20}\text{Ne}$ .....	7.9	4.0- <sup>d</sup>	17.9	M17.9 <sup>d</sup>	33.3 <sup>c</sup>	33.3 <sup>d</sup>	43.0 <sup>c</sup>	43.0 <sup>d</sup>
$^{22}\text{Ne}$ .....	5.0	1.5-	17.0	10.2-	15.7	7.9-	18.4	23.9+
$^{23}\text{Na}$ .....	5.6	3.1-	14.3	11.0-	13.5	13.6	17.5	26.3+
$^{24}\text{Mg}$ .....	5.5	4.4- <sup>d</sup>	12.4	11.2- <sup>d</sup>	12.2	16.7+ <sup>d</sup>	16.5	25.6+ <sup>d</sup>
$^{25}\text{Mg}$ .....	4.7	2.7-	11.9	8.9-	11.1	11.2	14.5	21.1+
$^{26}\text{Mg}$ .....	3.8	1.9-	11.6	7.0-	10.4	6.8-	12.6	17.6+
$^{27}\text{Al}$ .....	4.0	2.3-	9.8	7.3-	9.2	9.9+	11.9	16.4+
$^{28}\text{Si}$ .....	3.8	2.6-	8.5	7.7-	8.3	11.2+ <sup>d</sup>	11.2	16.8+ <sup>d</sup>
$^{32}\text{S}$ .....	2.6	1.6-	5.9	5.0-	5.6	7.3+	7.6	10.6+
$^{56}\text{Fe}$ .....	1.0	0.1-	1.6	0.4-	0.8	0.4-	0.8	0.8

<sup>a</sup> Units are millibarns. S is for Saclay and UNH is for University of New Hampshire.

<sup>b</sup> Plus and minus signs indicate direction of change over Saclay-modified TS cross sections.

<sup>c</sup> Modified from TS.

<sup>d</sup> Directly measured cross sections.

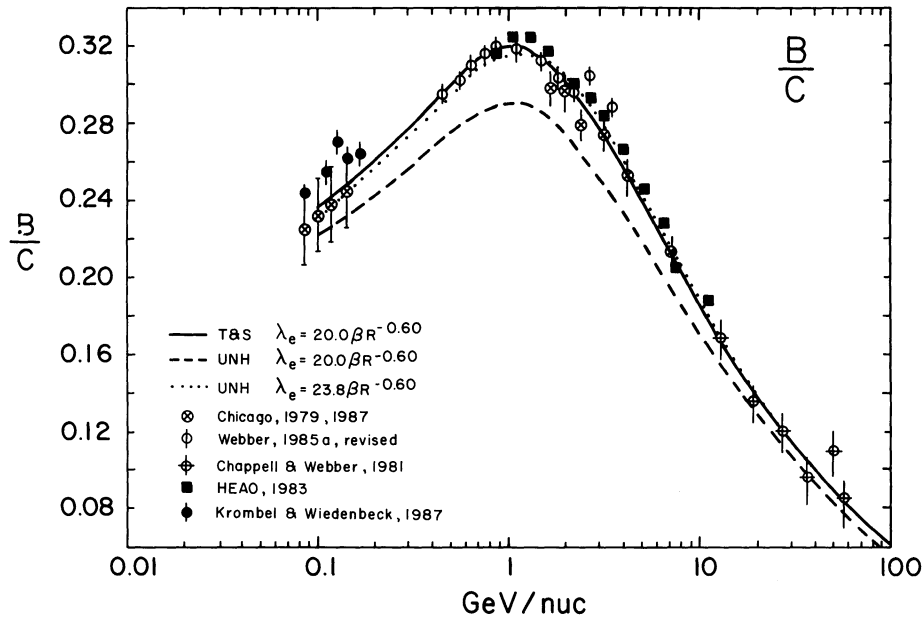


FIG. 1.—The B/C ratio vs. kinetic energy shown for the following cases: *solid line*, path length  $\lambda_e = 20.0 \beta R^{-0.6}$  for  $R > 4.5$  GV,  $\lambda_e = 8.1 \beta \text{ g cm}^{-2}$  for  $R < 4.5$  GV, Scalay-modified  $T$  and  $S$  cross sections; *dashed line*, same path length, UNH cross sections; *dotted line*, path length  $\lambda_e = 23.8 \beta R^{-0.6}$  for  $R > 4.5$  GV,  $\lambda_e = 9.7 \beta \text{ g cm}^{-2}$  for  $R < 4.5$  GV, UNH cross sections.

#### IV. THE COSMIC-RAY MEASUREMENTS

Essentially, measurements of the boron and nitrogen abundances have been made in two ways:

1. *Elemental observations of the B/C and N/O ratios (Figs. 1 and 2).*—Here, the most recent and accurate high-energy measurements are those made aboard the *HEAO 3* C-2 satellite in the energy range 0.7–15 GeV nucleus<sup>-1</sup>, as in Engelmann *et al.* (1983). Also included are measurements recently reported by Dwyer and Meyer (1985) and higher energy measurements from the work of Chappell and Webber (1981). At low energies, balloon measurements made by Webber, Kish, and Schrier (1985a) in the energy range 0.3–4.0 GeV nucleus<sup>-1</sup>, *IMP 8* data by the Chicago group (Garcia-Munoz *et al.* 1979) in the energy range 70–280 MeV nucleus<sup>-1</sup>, and *ISEE 3* data from Krombel and Wiedenbeck (1987) are used.

2. *Isotopic measurements of N (Figs. 3 and 4).*—Currently acceptable isotopic measurements of nitrogen at low energies cover the range from 50 MeV nucleus<sup>-1</sup> to about 500 MeV nucleus<sup>-1</sup>. Included here are data obtained by Mewaldt *et al.* (1981) from an

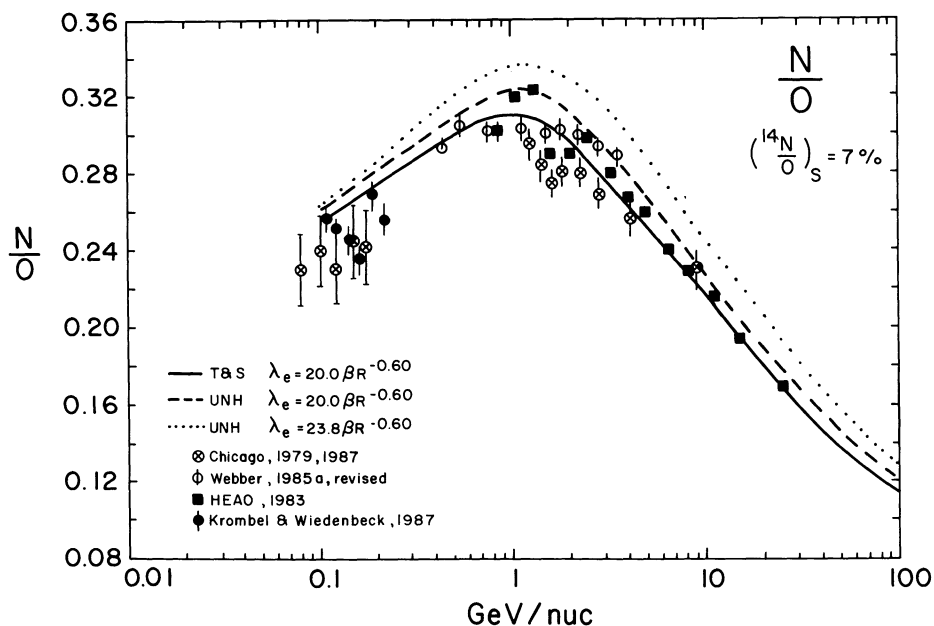


FIG. 2.—The N/O elemental ratio for the same parameters as in Fig. 1. The  $^{14}\text{N}/\text{O}$  source ratio is assumed to be 7%.

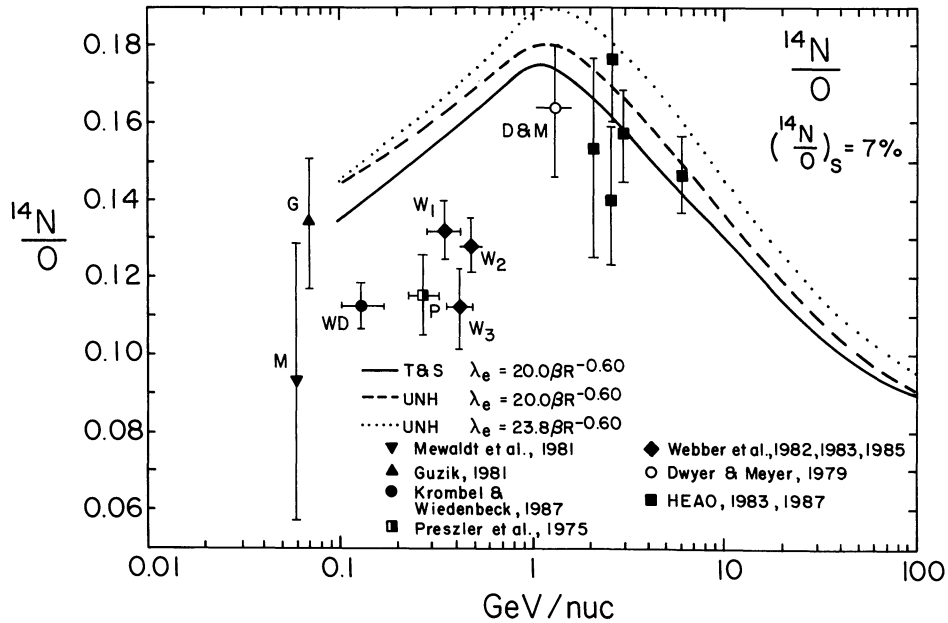


FIG. 3.—The  $^{14}\text{N}/\text{O}$  isotopic ratio for the same parameters as in Fig. 1. The  $^{14}\text{N}/\text{O}$  source ratio is assumed to be 7%.

instrument aboard the *ISEE 3* satellite in the energy range 30–130 MeV nucleus $^{-1}$ . Measurements from 80–230 MeV nucleus $^{-1}$  made by Krombel and Wiedenbeck (1987) on *ISEE 3* are also shown. Data gathered by Guzik (1981) on the elemental and isotopic composition of Galactic cosmic-ray N nuclei from 45–211 MeV nucleus $^{-1}$  from instruments aboard the *IMP 7* and *IMP 8* satellites are also used. Balloon data obtained by Preszler *et al.* (1975) and Webber (1982*b*, 1983) and Webber, Kish, and Schrier (1985*b*) with quoted errors are also shown.

Isotopic measurements of nitrogen at higher energies have all been made using the geomagnetic cut-off technique which permits only the determination of a mean mass. Results include those of Dwyer and Meyer (1979) at  $\sim 1.2$  GeV nucleus $^{-1}$  and a series of measurements using the *HEAO 3 C-2* spacecraft which are not all independent (Byrnak *et al.* 1983; Goret *et al.* 1983; Soutoul *et al.* 1983; Ferrando *et al.* 1988) in the energy range 2–7 GeV nucleus $^{-1}$ . These high-energy measurements may still be affected by systematic errors, especially for N (see Ferrando *et al.* 1988).

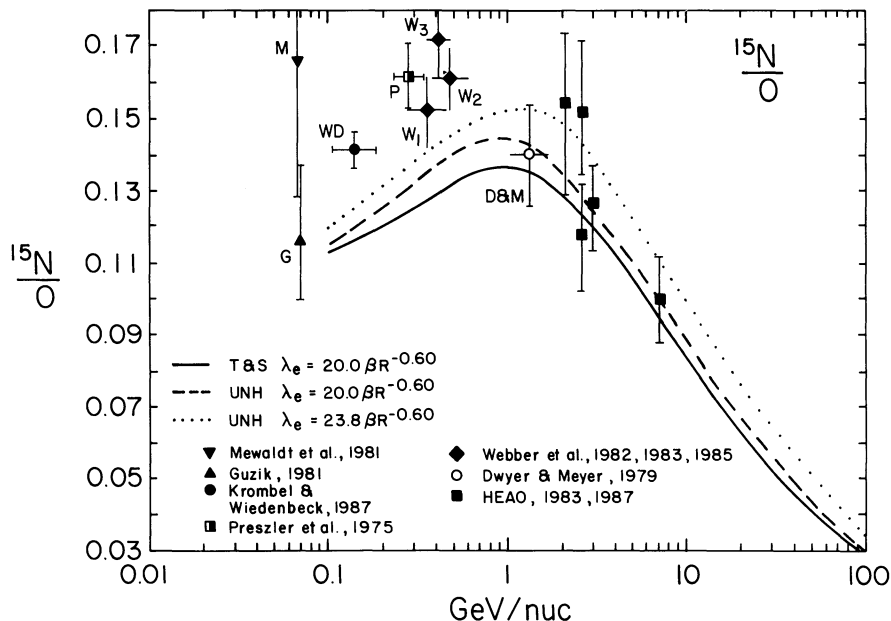


FIG. 4.—The  $^{15}\text{N}/\text{O}$  isotopic ratio for the same parameters as in Fig. 1. The  $^{15}\text{N}/\text{O}$  source ratio is assumed to be zero.



## V. THE CALCULATIONS

First, the Saclay modified TS cross sections were introduced into our propagation program to calculate the B/C ratio, and this was used as a reference. The best fit to the measurements using these cross sections was achieved with an escape path length  $\lambda_e = 20.0 \beta R^{-0.60}$  for  $R > 4.5$  GV and  $\lambda_e = 8.1 \beta \text{ g cm}^{-2}$  for  $R < 4.5$  GV (Figs. 1–4; solid lines in all figures) for a modulation parameter  $\phi = 450$  MV ( $R$  is the magnetic rigidity in GV).

The observed elemental N/O ratio is expected to be reproduced by using the same path length, although due to the presence of  $^{14}\text{N}$  at the source, the source abundance is a free parameter in the calculation. Figure 2 shows that a reasonable fit does indeed result at all energies for a source ratio N/O = 7%. However, the  $^{15}\text{N}/\text{O}$  isotopic ratio (Fig. 4), which is independent of this source abundance, instead of being simultaneously fitted along with the B/C ratio, is underpredicted by as much as 30% at low energies. At low energies the  $^{14}\text{N}/\text{O}$  isotopic ratio (Fig. 3) is overpredicted if a source abundance of 7% is assumed (the data favor a lower source abundance of  $\sim 3\%$ ). At high energies, the best fit to the  $^{14}\text{N}/\text{O}$  isotopic ratio is obtained for a source ratio of 7%, although the scatter of the data points is large. As we have seen, this fraction is also indicated by the elemental N/O ratio (Fig. 2). This value of elemental N/O<sub>s</sub> = 7% is inconsistent with the value of 3% derived from isotopic  $^{14}\text{N}/\text{O}$  measurements at low energies.

The next step in our calculation was to run the propagation program with the new UNH cross sections using the above escape length. The results of these calculations are plotted as dashed lines in Figures 1–4 for all four ratios being considered here: B/C, N/O,  $^{14}\text{N}/\text{O}$ , and  $^{15}\text{N}/\text{O}$ . When compared with calculations using the old cross sections, the predicted B/C ratio (Fig. 1, *dashed line*) is seen to *decrease* by 9% at 1 GeV nucleus<sup>-1</sup>, with similar decreases in all other energies. At the same time, the N/O ratio is observed to *increase* at the same energy by about 4% (Fig. 2). Again, at 1 GeV nucleus<sup>-1</sup>, both isotopic N ratios are seen to increase using the UNH cross sections: the increase being about 2% for the  $^{14}\text{N}/\text{O}$  ratio and about 6% for the  $^{15}\text{N}/\text{O}$  ratio (Figs. 3 and 4). These changes are almost entirely due to differences in the cross sections into B and N nuclei from nuclei heavier than  $^{16}\text{O}$ , or neutron-rich parents such as  $^{13}\text{C}$  and  $^{15}\text{N}$ , since the UNH cross sections for  $^{16}\text{O}$  and  $^{12}\text{C}$  into B and N were already included in the Saclay set of cross sections.

Clearly, the B/C ratio used as a reference needs to be refitted to the experimental data when the complete series of UNH cross sections are used. In order to do so, it is necessary to increase the escape path length by about 18% at 1 GeV nucleus<sup>-1</sup>. The new value is  $\lambda_e = 23.8 \beta R^{-0.60}$  for  $R > 4.5$  GV and  $\lambda_e = 9.7 \beta \text{ g cm}^{-2}$  for  $R < 4.5$  GV, with the same solar modulation factor. These new calculations are shown as dotted lines in Figures 1–4.

Now, the overall increase in the N/O elemental ratio is seen to be 8% over predictions made using the old cross sections and the smaller escape path length. The  $^{14}\text{N}/\text{O}$  isotopic ratio is also seen to increase by a total of about 8%. The increase in the  $^{15}\text{N}/\text{O}$  ratio is  $\sim 11\%$  above the earlier value at 1 GeV nucleus<sup>-1</sup> (Figs. 3 and 4). Table 2 summarizes the above results at 1 GeV nucleus<sup>-1</sup>.

As a result, an overprediction in the elemental N/O ratio now exists if the source abundance of nitrogen is kept equal to  $\sim 7\%$ .

VI. THE NEW  $^{14}\text{N}$  SOURCE ABUNDANCE

As the final step in our calculations, the source abundance of  $^{14}\text{N}$  (a free parameter thus far) was varied. The reader is referred to Figures 5–8, where propagation calculations are carried out using UNH cross sections, the new path length, and new source abundances. It is seen that a best fit to the elemental N/O ratio (Fig. 6) is now achieved at all energies when  $^{14}\text{N}/\text{O}|_s \simeq 3.8 \pm 1.0\%$ . For isotopic  $^{14}\text{N}/\text{O}$  ratio the best overall fit is also achieved by assuming a 3.8% source abundance (Fig. 7). This fit is in marginal agreement with both the low-energy data (somewhat high) and the high-energy data (somewhat low) which, however, scatter a lot and may still be affected by systematic errors.

Turning next to the  $^{15}\text{N}/\text{O}$  ratio, we see that some difficulties still exist, although fewer than previously. As may be seen from Figure 8, the  $^{15}\text{N}/\text{O}$  ratio is still underpredicted by  $\sim 10\%$ – $15\%$  at low energies. In the high-energy range, the predictions are within  $1 \sigma$  of the errors as quoted by the experimenters themselves for four of the six data points. Figure 8 shows that a much better fit would be achieved in the absence of a  $\beta$  dependence of  $\lambda_e$  which is, however, not acceptable when the other ratios are considered.

A lower  $^{14}\text{N}$  source abundance along with new cross sections does indeed help to resolve some puzzles mentioned earlier:

1. Estimates of  $^{14}\text{N}/\text{O}|_s$  derived from both low- and high-energy isotopic  $^{14}\text{N}/\text{O}$  observations and from all elemental N/O observations are now consistent with the same source ratio of 3.8%.

2. The expected simultaneous fit of the observed B/C and  $^{15}\text{N}/\text{O}$  ratios is not entirely achieved at low energies. We maintain, however, that an improved fit is obtained for the same set of parameters that fit the B/C ratio. The existing difference between predictions and measurements in this case, 10%–15% at low energies, is now comparable to experimental uncertainties in the measurements or uncertainties due to unmeasured cross sections, and suggests a ratio  $^{15}\text{N}/\text{O}|_s \leq 1\%$  and consistent with zero.

TABLE 2  
CALCULATED RATIOS AND PERCENTAGE DIFFERENCES IN RATIOS AT 1 GeV NUCLEUS<sup>-1</sup>

Ratio	Saclay	UNH(1)	Percent Difference (Saclay–UNH[1])	UNH(2)	Percent Difference (Saclay–UNH[2])
B/C.....	0.321	0.292	9–	0.316	2–
N/O.....	0.313	0.325	4+	0.338	8+
$^{14}\text{N}/\text{O}$ ..	0.176	0.179	2+	0.189	8+
$^{15}\text{N}/\text{O}$ ..	0.137	0.145	6+	0.152	11+

NOTE.—UNH(1) indicates  $\lambda_e = 20.0 \beta R^{-0.60}$  for  $R > 4.5$  GV and  $\lambda_e = 8.1 \beta \text{ g cm}^{-2}$  for  $R < 4.5$  GV. UNH(2) indicates  $\lambda_e = 23.8 \beta R^{-0.60}$  for  $R > 4.5$  GV and  $\lambda_e = 9.7 \beta \text{ g cm}^{-2}$  for  $R < 4.5$  GV. Signs after numbers indicate increase (+) or decrease (–) over Saclay values.

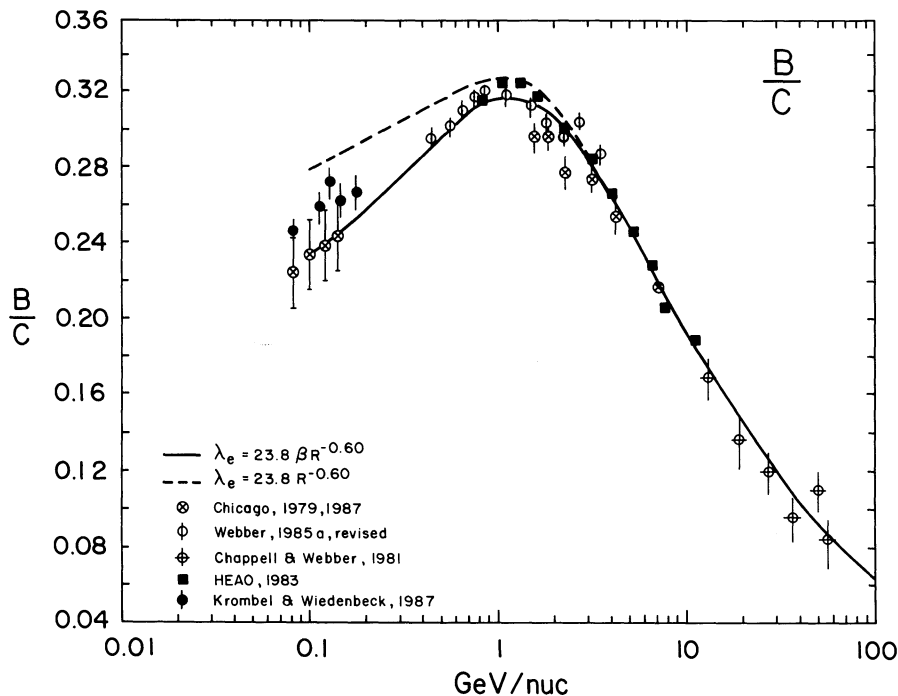


FIG. 5.—The B/C ratio obtained using the new path length and UNH cross sections. Dashed line shows results with no  $\beta$  dependence of the path length.

#### VII. STELLAR NUCLEOSYNTHESIS AND THE NEW $^{14}\text{N}$ SOURCE ABUNDANCE

To be identified are possible sources or astrophysical sites consistent with the low  $^{14}\text{N}$  abundance we have determined. The smallness of this value is clearly evident when seen in comparison to measurements of this ratio in other astronomical regions. The solar energetic particle (SEP) value for  $\text{N}/\text{O} = 12.5\%$ , from which Breneman and Stone (1985) obtained “SEP-derived photospheric and coronal” ratios of 12.1% and 12.3%, respectively. Direct spectroscopic measurements yield  $\text{N}/\text{O} = 11.7\%$  for the photosphere (Grevesse 1984) and 16%, within a factor of 2, for the corona (Meyer 1985a). In addition, the local Galactic (LG) abundance of  $\text{N}/\text{O} = 10\%$  (Meyer 1985a), which is in agreement with observations of the Orion Nebula situated at 10.4 kpc from the Galactic center (or 0.4 kpc from the Sun) (Peimbert and Tores-Peimbert 1977; Mewaldt *et al.* 1981), while optical observations of our galaxy

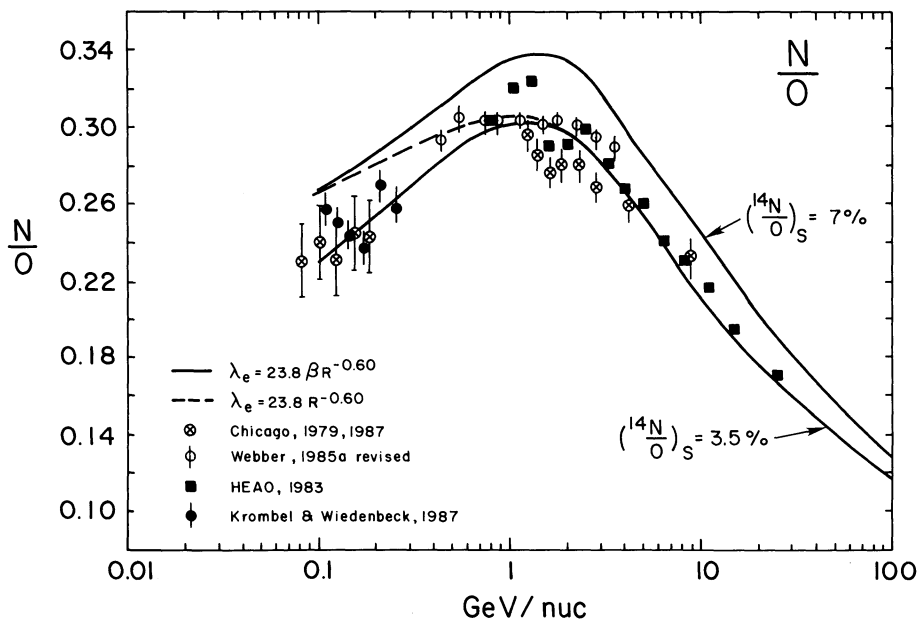


FIG. 6.—The N/O elemental ratio obtained using the new path length and UNH cross sections for  $^{14}\text{N}/\text{O}$  source abundances of 3.5% and 7%. Dashed line as in Fig. 5.

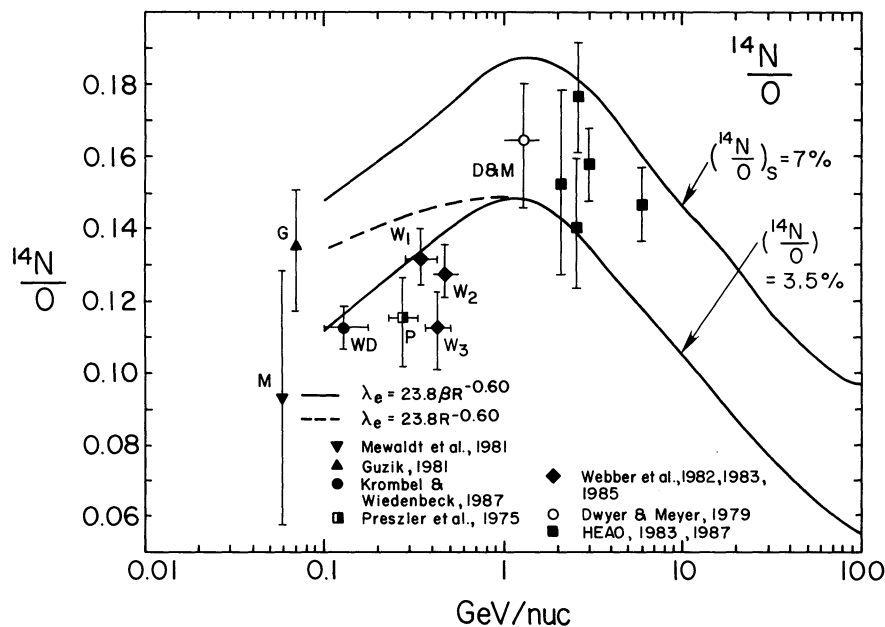


FIG. 7.—The  $^{14}\text{N}/\text{O}$  isotopic ratio obtained using the new path length and UNH cross sections for  $^{14}\text{N}/\text{O}$  source abundances of 3.5% and 7%. Dashed line as in Fig. 5.

show no large galactocentric gradient with regard to this ratio (Pagel 1985, and references therein). It is evident then that N in the cosmic-ray source is indeed depleted relative to O, for some reason, relative to most other astrophysical sources by a factor of 3 or 4. It must be noted that the first ionization potentials (FIPs) of N and O are in fact very similar: 14.5 eV and 13.6 eV, respectively. We believe, in agreement with Cassé and Goret (1978), that, although the FIP in some cases may serve to explain the differences between Galactic cosmic rays (GCRs) and the solar system composition, it is unlikely to be of importance here. Thus an underabundance of N relative to O, when compared with SEPs or LG abundances, could be one of the best indicators for understanding the types of sources that produce cosmic rays and may imply that cosmic rays are produced by a nucleosynthetic process that differs in important respects from that of the bulk of solar system matter. In fact, various models have already been put forward to explain an underabundance of N in cosmic rays (see, for example, Cassé [1981] for a summary), but few predict N/O ratios as low as 4%. The only class of models we are aware of which might predict such a low abundance are the models of Woosley and Weaver (1982) for

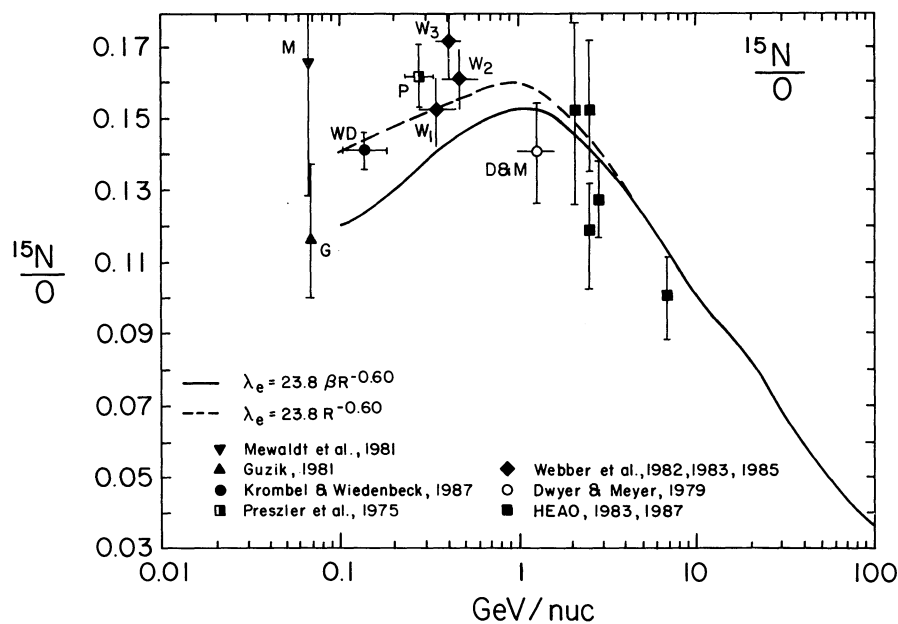


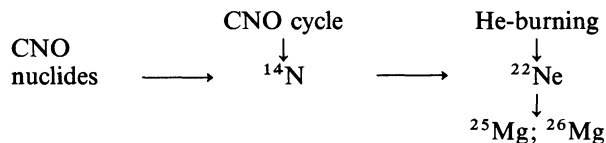
FIG. 8.—The  $^{15}\text{N}/\text{O}$  isotopic ratio obtained using the new path length and UNH cross sections for a  $^{15}\text{N}/\text{O}$  source abundance of zero. Dashed line shows results with no  $\beta$  dependence of the path length.

nucleosynthesis in stars  $\sim 25 M_{\odot}$  which may become Type II supernova. These models utilize the mixing of supernova ejecta, which is poor in  $^{14}\text{N}$ , with interstellar material which is richer in  $^{14}\text{N}$  to obtain the final abundance values. However, these abundances do not reproduce the singularly important differences in  $^{12}\text{C}$  and  $^{22}\text{Ne}$  abundances observed in Galactic cosmic rays since the production of  $^{12}\text{C}$  in these models is low when compared with that of  $^{16}\text{O}$ , whereas in cosmic rays the reverse is true. This is not necessarily a problem, since additional  $^{12}\text{C}$  could be produced in lower mass stars, but as a consequence two kinds of models are required to explain the differences.

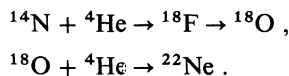
The generally accepted belief is that, in massive stars which have undergone and completed the CNO cycle,  $^{14}\text{N}$  exists at the onset of the He-burning phase as the original C–N–O abundance. At the onset of He-burning, the  $^{14}\text{N}$  gets converted into  $^{18}\text{O}$  and then rapidly into  $^{22}\text{Ne}$ . The end result is that matter ejected from the He-burning zone is enriched in  $^{22}\text{Ne}$  (and  $^{12}\text{C}$ ), a fact that is model-independent (Meyer 1985a). These and related facts have led researchers to consider Wolf-Rayet (WR) stars as possible sources of cosmic rays (Cassé and Paul 1982). The mechanics of WR stars models are beyond the scope of this paper, but the interested reader is referred to Gupta (1987) and references therein for details relevant to the present problem. Clearly, the success of a particular model would depend largely on its ability to reproduce accurately the observed charge and isotopic composition of Galactic cosmic rays. No existing model thus far has done so in a completely satisfactory way if  $^{14}\text{N}$  is indeed deficient.

It has been known for some time that the most important elemental and isotopic differences between the relative abundances of Galactic cosmic-ray sources and solar coronal (or SEP) material are for  $^{12}\text{C}$ ,  $^{22}\text{Ne}$ ,  $^{25}\text{Mg}$ , and  $^{26}\text{Mg}$  and possibly  $^{16}\text{O}$  and  $^{29}\text{Si}$  and  $^{30}\text{Si}$  in addition to  $^{14}\text{N}$  (e.g., Wiedenbeck 1984; Meyer 1985a) (since with respect to the solar photosphere or meteorites the well-known FIP effect is dominant). These differences have prompted Meyer (1985b) and others to suggest that a significant fraction of the Galactic cosmic rays might originate primarily in He-burning zones, such as those associated with massive stars. These differences would then be due to nucleosynthetic effects, rather than to atomic selection processes such as the FIP. Specifically, the problem we now address is as follows:

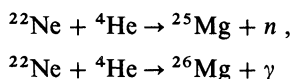
$^{14}\text{N}$  occurs as a result of He-burning in the nucleosynthetic reaction chain as follows:



An enhancement of  $^{22}\text{Ne}$  would be expected to arise as a result of the burning of this locally synthesized  $^{14}\text{N}$ , e.g.,



As we have noted, cosmic-ray isotope measurements have indicated enhancements relative to solar system abundances in the source abundances of other neutron-rich isotopes such as those of the “second generation,” which include  $^{25}\text{Mg}$  and  $^{26}\text{Mg}$  produced by



(Audouze and Vauclair 1979), and thus dependent on the amount of  $^{22}\text{Ne}$  produced. At this same stage  $^{12}\text{C}$  is turned into  $^{16}\text{O}$  via  $^{12}\text{C} + ^4\text{He} \rightarrow ^{16}\text{O} + \gamma$ , so that some  $^{16}\text{O}$  excess might also be expected associated with a  $^{25,26}\text{Mg}$  excess. If such a scenario is followed, we might expect that since a depletion of  $^{14}\text{N}$  is observed and an enhancement of  $^{22}\text{Ne}$  and  $^{25,26}\text{Mg}$  is also observed in cosmic rays these abundance differences might be a manifestation of the He-burning process.

#### VIII. A QUANTITATIVE EXAMINATION OF THE OVERABUNDANCE OF THE NEUTRON-RICH ISOTOPES $^{22}\text{Ne}$ , $^{25}\text{Mg}$ , AND $^{26}\text{Mg}$ AND THE UNDERABUNDANCE OF $^{14}\text{N}$ IN COSMIC RAYS WITH RESPECT TO THE SOLAR CORONA

We will proceed at this point to compare the underabundance of  $^{14}\text{N}$  with the overabundance of ( $^{22}\text{Ne} + ^{25}\text{Mg} + ^{26}\text{Mg}$ ) in cosmic rays with respect to their solar corona abundances.

Table 3 shows the relative abundances of various isotopes measured in the Galactic cosmic-ray source (GCR), the solar corona (SC), and the LG (essentially solar photospheric). All abundances are normalized to  $^{28}\text{Si}$ . We are using for our cosmic-ray source abundances new values obtained by our propagation calculations carried out using the new UNH cross sections in conjunction with the *HEAO 3* relative abundances (Engelmann *et al.* 1983). In this table both separate charge and isotopic fraction abundance determinations are used in combination so that the footnotes c and e, for example, represent the Breneman and Stone (1985) solar coronal charge composition derived from SEP combined with the isotope fractions also deduced from SEP by Mewaldt and Stone (1987). Errors are not shown on the ratios in Table 3 except for selected ones important for our arguments, because they are generally difficult to evaluate in a consistent fashion for the different types of sources. They are generally less than 10%, but may be larger in several cases—e.g., the local Galactic Ne abundance. The differences between the Mg isotope fractions for the SC given by Anders and Ebihara (1982) (terrestrial) and Mewaldt and Stone (1987) (derived from SEP) are probably only marginally significant. We have attempted to provide our best estimate of the combined effects of these errors on the data points in Figures 9 and 10.

From the usual plot of the GCR/LG abundance ratios versus the FIP (in Fig. 9), we see that there is a clear depletion as expected for elements with ionization potentials  $\geq 10$  eV (e.g., Goret *et al.* 1981; Mewaldt 1981; Meyer 1985a). The depletion factor for high-ionization potential elements is  $\sim 0.2$ , assuming a step function at  $\sim 10$  eV (e.g., Webber, Kish, and Schrier 1985b). Since we



TABLE 3  
ISOTOPIC ABUNDANCES OF ELEMENTS (NORMALIZED TO  $^{28}\text{Si}$ )

Isotope	GCR <sup>a</sup>	SC	LG, Photosphere
$^{12}\text{C}$ .....	4.638	2.550 <sup>b</sup>	14.77 <sup>c</sup>
$^{14}\text{N}$ .....	$0.220 \pm 0.058$	$0.760 \pm 0.056^b$	2.93 <sup>c</sup>
$^{16}\text{O}$ .....	5.796	6.160 <sup>b</sup>	25.17 <sup>c</sup>
$^{20}\text{Ne}$ .....	0.466	0.750 <sup>b,e</sup> (0.791 <sup>b,d</sup> )	3.33 <sup>b,c</sup>
$^{21}\text{Ne}$ .....	<0.016	<0.011 <sup>b,e</sup>	0.008 <sup>b,c</sup>
$^{22}\text{Ne}$ .....	$0.207 \pm 0.015$	0.099 <sup>b,e</sup> (0.059 <sup>b,d</sup> )	0.243 <sup>b,c</sup>
Ne $\Sigma$ .....	0.6743	0.851 <sup>b,e</sup> (0.851 <sup>b,d</sup> )	3.581 <sup>c</sup>
$^{24}\text{Mg}$ .....	0.833	0.884 <sup>b,e</sup> (0.932 <sup>b,d</sup> )	0.913 <sup>b,c</sup>
$^{25}\text{Mg}$ .....	$0.135 \pm 0.020$	0.142 <sup>b,e</sup> (0.118 <sup>b,d</sup> )	0.118 <sup>b,c</sup>
$^{26}\text{Mg}$ .....	$0.163 \pm 0.020$	0.154 <sup>b,e</sup> (0.130 <sup>b,d</sup> )	0.130 <sup>b,c</sup>
Mg $\Sigma$ .....	1.1311	1.180 <sup>b</sup> (1.180) <sup>c</sup>	1.160 <sup>c</sup>
$^{28}\text{Si}$ .....	1.000	1.000 <sup>b,d</sup>	1.000 <sup>b,c</sup>
$^{29}\text{Si}$ .....	0.071	0.051 <sup>b,d</sup>	0.051 <sup>b,c</sup>
$^{30}\text{Si}$ .....	0.034	0.034 <sup>b,d</sup>	0.034 <sup>b,c</sup>
Si $\Sigma$ .....	1.1046	1.085 <sup>b</sup>	1.085 <sup>c</sup>

<sup>a</sup> Latest source abundances derived using the UNH cross sections and new escape length.

<sup>b</sup> Breneman and Stone 1985. (Elements from SEP.)

<sup>c</sup> Meyer 1987*b*. (Elements.)

<sup>d</sup> Anders and Ebihara 1982. (Isotopes: solar wind for Ne, terrestrial for Mg and Si.)

<sup>e</sup> Mewaldt and Stone 1987. (Isotopes: from SEP for Ne and Mg.)

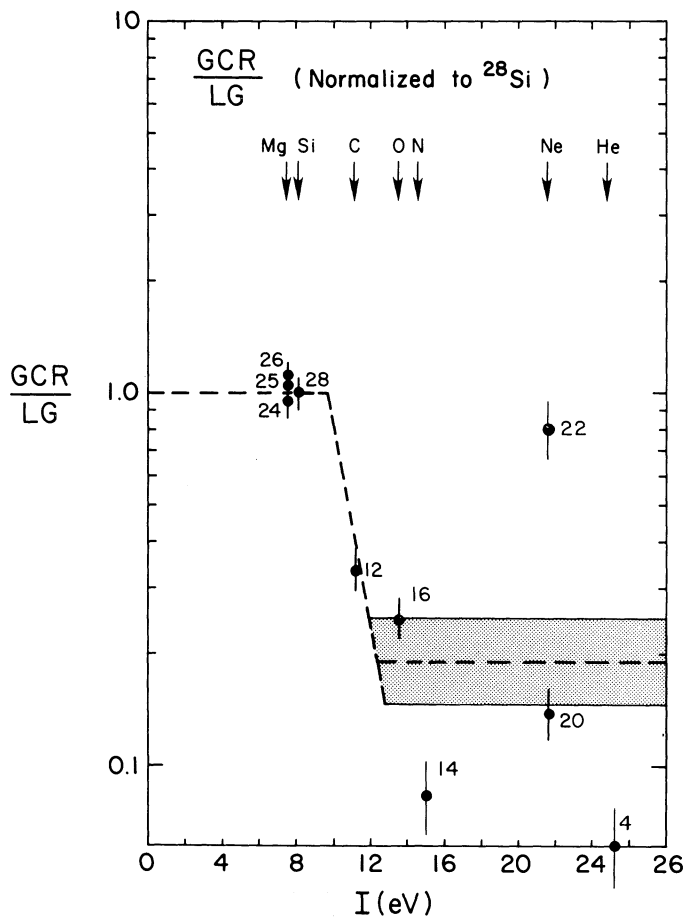


FIG. 9.—The ratio of cosmic-ray source abundances/local Galactic (or solar photospheric) abundances vs. FIP (from data in Table 3). Isotope ratios are from Anders and Ebihara (1982).

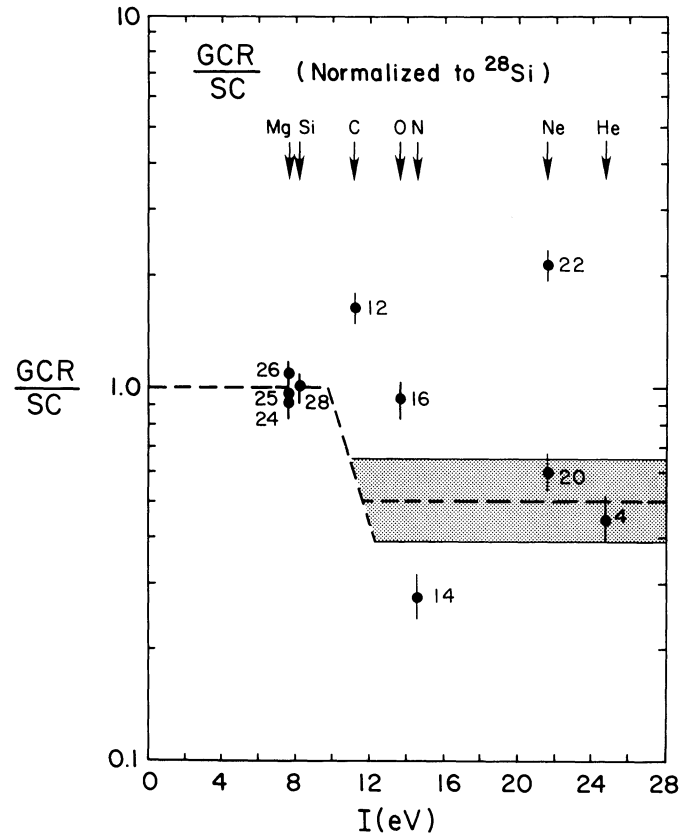


FIG. 10.—The ratio of cosmic-ray source abundances/solar coronal abundances vs. FIP (from data in Table 3). Isotope ratios are from Anders and Ebihara (1982).

have no reason to expect that, *a priori*, our cosmic-ray source abundance will resemble the solar corona or solar energetic particle abundances rather than the LG abundances, it may be more interesting to compare the cosmic-ray source abundances with those of the solar corona. Figure 10 shows the GCR/SC ratios for various elements and isotopes versus the ionization potentials of each. In this comparison we no longer observe a systematic depletion of all elements or isotopes of high ionization potentials. This difference between the GCR/LG and GCR/SC ratios is well known and is related, in part, to solar coronal fractionation with respect to the solar photosphere and related to the FIP (e.g., Breneman and Stone 1985). In the GCR/SC comparison, an enhancement of  $^{12}\text{C}$ , and possibly  $^{16}\text{O}$  and the neutron-rich isotope,  $^{22}\text{Ne}$ , exists along with a depletion of  $^{14}\text{N}$  and possibly  $^{20}\text{Ne}$  relative to  $^{28}\text{Si}$ . We are led to believe, in light of this, that some other processes in addition to the FIP might be occurring that bring about the difference between these two types of sources.

To study these additional differences with respect to the SC we will correct our GCR abundances of  $^{14}\text{N}$  and  $^{22}\text{Ne}$  for a FIP-related depletion factor of 0.5 with respect to  $^{28}\text{Si}$  as derived from the points for  $^{20}\text{Ne}$  and  $^4\text{He}$  in Figure 10. ( $^{20}\text{Ne}$  is indeed likely to remain unaffected by the nucleosynthetic process we will consider below; see also Webber, Kish, and Schrier 1985*b*.) Using these corrected cosmic-ray source abundances, the solar coronal elemental abundance estimates of Breneman and Stone (1985), and isotopic fractions from Anders and Ebihara (1982) (which are solar wind data for Ne and terrestrial for Mg) (see Table 3), we compare the GCR  $^{14}\text{N}$  deficiency with respect to the SC (using  $^{28}\text{Si}$  as a reference),

$$(\text{SC} - \text{GCR}/0.5)_{^{14}\text{N}} \times ^{28}\text{Si} = (0.320 \pm 0.109) \times ^{28}\text{Si} ,$$

to the  $^{22}\text{Ne} + ^{25}\text{Mg} + ^{26}\text{Mg}$  excess,

$$[(\text{GCR}/0.5 - \text{SC})_{^{22}\text{Ne}} + (\text{GCR} - \text{SC})_{^{25}\text{Mg}} + \text{GCR} - \text{SC}]_{^{26}\text{Mg}} \times ^{28}\text{Si} = [0.356 + 0.017 + 0.033] \times ^{28}\text{Si} = (0.406 \pm 0.056) \times ^{28}\text{Si} .$$

We see that, compared to SC abundances, the depletion of  $^{14}\text{N}$  is roughly balanced by the overabundance of the neutron-rich isotopes  $^{22}\text{Ne}$ ,  $^{25}\text{Mg}$ , and  $^{26}\text{Mg}$ .

If, on the other hand, we use the solar coronal isotopic fractions for Ne and Mg derived from SEP by Mewaldt and Stone (1987) rather than the solar isotopic fractions of Anders and Ebihara (1982) then we find, for the  $^{14}\text{N}$  deficiency,  $(0.320 \pm 0.109) \times ^{28}\text{Si}$  and, for the  $^{22}\text{Ne} + ^{25}\text{Mg} + ^{26}\text{Mg}$  excess,  $(0.315 - 0.007 + 0.009) \times ^{28}\text{Si} = (0.317 \pm 0.056) \times ^{28}\text{Si}$ —the  $^{14}\text{N}$  depletion is now almost exactly balanced by the  $^{22}\text{Ne}$  enhancement—but also now  $^{25}\text{Mg}$  and  $^{26}\text{Mg}$  are no longer significantly enhanced in the cosmic-ray source relative to the solar corona.

We believe that, based on the above analysis, there appears to be a direct correspondence between the excess of the neutron-rich isotope  $^{22}\text{Ne}$ , and possibly  $^{25}\text{Mg}$  and  $^{26}\text{Mg}$ , and the depletion of  $^{14}\text{N}$  in cosmic rays with respect to the SC abundances.

## IX. CONCLUSIONS

The results of this paper suggest the following:

1. Atomic selection effects alone cannot explain adequately the observed depletion of  $^{14}\text{N}$  relative to  $^{16}\text{O}$  in the cosmic-ray source with respect to the solar corona by a factor of  $\sim 3$ ; thus at least some part of this depletion must have a nuclear/nucleosynthetic origin. Part of this anomaly may be due to an enhancement of  $^{16}\text{O}$  by a factor  $\sim 1.5$  due to the He-burning component.
2. The overabundance of  $^{22}\text{Ne}$ , and possibly  $^{25}\text{Mg}$  and  $^{26}\text{Mg}$ , in cosmic rays relative to the solar corona is almost exactly balanced by the depletion of  $^{14}\text{N}$ . Since in the He-burning process  $^{14}\text{N}$  is converted into  $^{22}\text{Ne}$  and  $^{25}\text{Mg}$  and  $^{26}\text{Mg}$ , this may suggest a connection between these two statements, although such a connection is not easily interpreted in terms of the normal nucleosynthesis occurring in massive stars as pointed out by Meyer (1987*a, b*).
3. If a comparison is made with the new solar coronal isotopic abundances derived by Mewaldt and Stone (1987) then *no enhancement of  $^{25}\text{Mg}$  and  $^{26}\text{Mg}$  in the cosmic-ray source is indicated by the data.*

This work was performed under NASA grant NGR 30-002-052.

## REFERENCES

- Anders, E., and Ebihara, M. 1982, *Geochim. Cosmochim. Acta*, **46**, 2363.
- Audouze, J., and Vauclair, S. 1979, *Geophys. Ap. Monographs*, Vol. **18** (Dordrecht: Reidel).
- Breneman, H. H., and Stone, E. C. 1985, *Ap. J. (Letters)*, **299**, L57.
- Byrnak, B., et al. 1983, *Proc. 18th Internat. Cosmic Ray Conf.*, **9**, 135.
- Cassé, M. 1981, *Proc. 17th Internat. Cosmic Ray Conf.*, **13**, 111.
- Cassé, M., and Goret, P. 1978, *Ap. J.*, **221**, 703.
- Cassé, M., and Paul, J. A. 1982, *Ap. J.*, **258**, 860.
- Chappell, J. H., and Webber, W. R. 1981, *Proc. 17th Internat. Cosmic Ray Conf.*, **2**, 59.
- Comstock, G. M. 1969, *Ap. J.*, **155**, 619.
- Cook, W. R., Stone, E. C., and Vogt, R. E. 1980, *Ap. J. (Letters)*, **238**, L97.
- Dwyer, R., and Meyer, P. 1979, *Proc. 16th Internat. Cosmic Ray Conf.*, **12**, 97.
- . 1985, *Ap. J.*, **294**, 441.
- Engelmann, J. J., et al. 1984, in *9th European Cosmic Ray Symposium*, ed. K. Kudela and S. Pinter (Kosice: Slovak Academy of Sciences), p. 141.
- Engelmann, J. J., et al. 1983, *Proc. 18th ICRC*, **2**, 17.
- Engelmann, J. J., et al. 1985, *Astr. Ap.*, **148**, 12.
- Ferrando, P., et al. 1988, *Astr. Ap.*, **193**, 69.
- Fichtel, C. E., and Reames, D. V. 1968, *Phys. Rev.*, **175**, 1564.
- Garcia-Munoz, M., Margolis, S., Simpson, J. A., Wefel, J. P. 1979, *Proc. 16th Internat. Cosmic Ray Conf.*, **1**, 310.
- Gleeson, L. J., and Axford, W. I. 1968, *Ap. J.*, **154**, 1011.
- Gloeckler, G., and Jokipii, J. R. 1969, *Phys. Rev. Letters*, **22**, 1448.
- Goret, P., et al. 1983, *Proc. 18th Internat. Cosmic Ray Conf.*, **9**, 139.
- Grevesse, N. 1984, *Frontiers of Astronomy and Astrophysics*, ed. R. Pallavian (Florence: Italian Astr. Soc.), p. 71.
- Gupta, M. 1987, Master's thesis, University of New Hampshire.
- Guzik, T. G. 1981, *Ap. J.*, **244**, 695.
- Koch-Miramond, L., et al. 1983, *Proc. 18th Internat. Cosmic Ray Conf.*, **9**, 275.
- Krombel, K. E., and Wiedenbeck, M. G. 1987, *Proc. 20th Internat. Cosmic Ray Conf.*, **2**, 26.
- Lund, N. 1984, *Adv. Space Res.*, Vol. **4**, Nos. 2-3, p. 5.
- Maeder, A., 1983*a*, *Astr. Ap.*, **120**, 113.
- . 1983*b*, *Astr. Ap.*, **120**, 130.
- Mewaldt, R. A. 1981, *Proc. 17th ICRC*, **13**, 49.
- Mewaldt, R. A., Spalding, J. D., Stone, E. C., and Vogt, R. E. 1981, *Ap. J. (Letters)*, **251**, L27.
- Mewaldt, R. A., and Stone, E. C. 1987, *Proc. 20th Internat. Cosmic Ray Conf.*, **3**, 255.
- Mayer, J. P. 1985*a*, *Ap. J. Suppl.*, **57**, 173.
- . 1985*b*, *Proc. 19th Internat. Cosmic Ray Conf.*, **9**, 141.
- . 1987*a*, in *Origin and Distribution of the Elements*, ed. G. J. Mathews (New Orleans: World Scientific), p. 310.
- . 1987*b*, in *Origin and Distribution of the Elements*, ed. G. J. Mathews (World Scientific), p. 337.
- Pagel, B. E. J., 1985, in *Proc. ESO Workshop on Production and Distribution of CNO elements* (Garching: ESO), p. 201.
- Preszler, A. M., Kish, J. C., Lezniak, J. A., Simpson, G., and Webber, W. R. 1975, *Proc. 14th ICRC*, **12**, 4096.
- Peimbert, M., and Torres-Peimbert, S. 1977, *M.N.R.A.S.*, **179**, 217.
- Soutoul, A., et al. 1983, *Proc. 18th Internat. Cosmic Ray Conf.*, **9**, 143.
- Tsao, C. H., and Silberberg, R. 1979, *Proc. 16th ICRC*, **2**, 202.
- Webber, W. R. 1975, *Proc. 14th ICRC*, **5**, 1597.
- . 1982*a*, *Ap. J.*, **252**, 386.
- . 1982*b*, *Ap. J.*, **255**, 329.
- . 1983, *Proc. 18th ICRC*, **9**, 151.
- . 1984, *Workshop on Cosmic Ray and High Energy  $\gamma$ -ray Experiments on the Space Station*, ed. W. V. Jones and J. P. Wefel (Baton Rouge: Louisiana State University Press), p. 283.
- . 1987*a*, *Proc. 20th ICRC*, **2**, 463.
- . 1987*b*, *Proc. 20th ICRC*, **8**, 65.
- . 1988, *Phys. Rev. C*, in press.
- Webber, W. R., and Gupta, M. 1987, *Proc. 20th ICRC*, **2**, 129.
- Webber, W. R., Gupta, M., Koch-Miramond, L., and Masse, P. 1985, *Proc. 19th ICRC*, **3**, 42.
- Webber, W. R., and Kish, J. C. 1985, *Proc. 19th ICRC*, **3**, 87.
- Webber, W. R., Kish, J. C., and Schrier, D. 1985*a*, *Proc. 19th ICRC*, **2**, 16.
- . 1985*b*, *Proc. 19th ICRC*, **2**, 88.
- Webber, W. R., Kish, J. C., and Schrier, D. 1987, *Proc. 20th ICRC*, **2**, 125.
- Wiedenbeck, M. E. 1984, *Adv. Space Res.*, **4**, 15.
- Woosley, S. E., and Weaver, T. A. 1982, in *Essays in Nuclear Astrophysics*, ed. C. A. Barnes, D. D. Clayton, and D. N. Schramm (Cambridge: Cambridge University Press), p. 377.

M. GUPTA and W. R. WEBBER: Space Science Center, EOS, 344 New Science Building, University of New Hampshire, Durham, NH 03824